Integrative genetic analysis of mouse and human AML identifies cooperating disease alleles

Megan A. Hatlen,[1,2,3,8] Kanika Arora,[9] Vladimir Vacic,[9] Ewa A. Grabowska,[9] Willey Liao,[9] Bridget Riley-Gillis,[9] Dayna M. Oschwald,[9] Lan Wang,[13,14] Jacob E. Joergens,[2,3] Alan H. Shih,[2,3] Franck Rapaport,[2,3] Shengqing Gu,[10,11] Francesca Voza,[2,3] Takashi Asai,[13,14] Benjamin G. Neel,[10,11,12] Michael G. Kharas,[1,6,7] Mithat Gonen,[4] Ross L. Levine,[2,3,5] and Stephen D. Nimer[13,14,15]

[1]Molecular Pharmacology Program, Sloan Kettering Institute, [2]Human Oncology and Pathogenesis Program, [3]Center for Epigenetics Research, [4]Epidemiology and Biostatistics, [5]Leukemia Service, Department of Medicine, [6]Center for Cellular Engineering, and [7]Center for Stem Cell Biology, Memorial Sloan Kettering Cancer Center, New York, NY 10065
[8]Weill Cornell Graduate School of Medical Sciences, New York, NY 10065
[9]New York Genome Center, New York, NY 10013
[10]Princess Margaret Cancer Center, University Health Network, Toronto, Ontario M5G 2M9, Canada
[11]Department of Medical Biophysics, University of Toronto, Toronto, Ontario M5G 1L7, Canada
[12]Laura and Isaac Perlmutter Cancer Center, New York University Langone Medical Center, New York, NY 10016
[13]Department of Biochemistry and Molecular Biology, [14]Sylvester Comprehensive Cancer Center, and [15]Department of Medicine, Miller School of Medicine, University of Miami, Miami, FL 33136

t(8;21) is one of the most frequent chromosomal abnormalities observed in acute myeloid leukemia (AML). However, expression of AML1-ETO is not sufficient to induce transformation in vivo. Consistent with this observation, patients with this translocation harbor additional genetic abnormalities, suggesting a requirement for cooperating mutations. To better define the genetic landscape in AML and distinguish driver from passenger mutations, we compared the mutational profiles of AML1-ETO–driven mouse models of leukemia with the mutational profiles of human AML patients. We identified TET2 and PTPN11 mutations in both mouse and human AML and then demonstrated the ability of *Tet2* loss and PTPN11 D61Y to initiate leukemogenesis in concert with expression of AML1-ETO in vivo. This integrative genetic profiling approach allowed us to accurately predict cooperating events in t(8;21)$^+$ AML in a robust and unbiased manner, while also revealing functional convergence in mouse and human AML.

4–12% of acute myeloid leukemia (AML) patients present with a translocation between chromosomes 8 and 21 (Müller et al., 2008). However, transgenic mice expressing AML1-ETO only develop AML after treatment with mutagenic agents, suggesting a requirement for cooperating events (Higuchi et al., 2002). Two mouse models of AML1-ETO–driven AML have been generated that may depend on the acquisition of such events for leukemogenesis. Expression of AML1-ETO in *Cdkn1a*-null cells or expression of AML1-ETO9a, a splice variant of AML1-ETO, in WT cells can induce fully penetrant AML after a prolonged latency (Yan et al., 2006; Peterson et al., 2007b). *CDKN1A* has never been found to be disrupted in t(8;21)$^+$ AML (Shiohara et al., 1997), suggesting that its loss does not functionally cooperate with AML1-ETO. Instead, it is thought that loss of CDKN1A in vivo prevents the repair of damaged DNA and allows for the accumulation of mutations and cooperating alleles in AML1-ETO$^+$ hematopoietic progenitors (McDonald et al., 1996). Studies of AML1-ETO9a–driven leukemia have found dysregulated expression of DNA repair genes (Alcalay et al., 2003), which might facilitate a similar acquisition of cooperating secondary events. We hypothesized that we could identify and credential disease alleles in t(8;21)$^+$ AML through integrative genomic studies of human AML and the mouse AMLs that arise from these models.

RESULTS AND DISCUSSION

Identification of phenotypically similar mouse models of t(8;21)$^+$ AML

We first expressed AML1-ETO or AML1-ETO9a in fetal liver cells isolated from WT or *Cdkn1a*$^{-/-}$ mice. All transplant recipients of AML1-ETO–expressing *Cdkn1a*$^{-/-}$ cells developed lethal AML with a median latency of 201 d. Expression of AML1-ETO9a in WT or *Cdkn1a*$^{-/-}$ cells resulted in a fully penetrant, lethal leukemia after a median latency of 175 and 196 d, respectively (Fig. 1 A). At euthanasia, leukemic mice had anemia, thrombocytopenia, and elevated white blood cell counts (Fig. 1 B). We observed blast cell accumulation in the bone marrow, liver, and spleen, resulting in splenomegaly

Correspondence to Stephen D. Nimer: snimer@med.miami.edu; or Ross L. Levine: leviner@mskcc.org

Abbreviations used: AML, acute myeloid leukemia; FDR, false discovery rate; SMG, significantly mutated gene; SNV, single nucleotide variant.

The Rockefeller University Press $30.00
J. Exp. Med. 2016 Vol. 213 No. 1 25–34
www.jem.org/cgi/doi/10.1084/jem.20150524

(Fig. 1, C and D). The GFP$^+$ blast cells display an immature immunophenotype; they are negative for lineage markers and SCA-1 but are c-KIT and MPO positive (Fig. 1 E and not depicted). Leukemia with an identical immunophenotype develops within secondary recipients (Fig. 1 F and not depicted). The observations that these mouse models are phenotypically similar and develop AML with similar penetrance and latency suggest that they have acquired similar secondary events.

Mouse models of AML reproduce the genomic landscape of human AML

We next investigated the mutational landscape of the mouse AMLs and compared it with somatic mutational analyses of other mouse AML models and AML patients (Stubbs et al., 2008; Cancer Genome Atlas Research Network, 2013). We did not observe a significant difference in the number of variants detected or genes targeted in the mouse models compared with AML patient samples (Fig. 2, A–C). When we restricted our analysis to genes for which human–mouse orthology is known, we observed a significant enrichment in mouse AML for specific genes (hypergeometric $P \leq 4.26 \times 10^{-20}$; Fig. 2 D) and protein domains (hypergeometric $P \leq 4.23 \times 10^{-3}$) mutated in human AML. The domains mutated in both human and mouse AML were similarly affected by recurrent mutations (Spearman correlation of domain p-values $r = 0.53$, $P \leq 2.73 \times 10^{-8}$; Fig. 2 E). We next investigated the frequency of mutations in different protein classes and found no differences in the protein classes targeted in AML1-ETO/AML1-ETO9a mouse AML versus human t(8;21)$^+$ AML ($P = 0.327$; Fig. 2 F).

Integrated genomic approach identifies potential cooperating events in t(8;21)$^+$ AML

We next sought to mine the mutational data to identify mutations capable of cooperating with AML1-ETO, focusing our efforts on the 424 genes mutated in both human and mouse AML and then further narrowing our focus to those genes that were also significantly mutated (defined as Genome MuSiC significantly mutated gene [SMG] false discovery rate [FDR] $\leq$ 30%). This reduced the number of potential candidates from 424 to 38 human genes, representing 45 mouse orthologues (Fig. 3 A). We focused on the mouse orthologues that were significantly mutated (FDR $\leq$ 10%) in AML1-ETO–driven leukemias, and not in MLL-AF9–driven leukemia, and identified 38 mouse genes that met these criteria (Fig. 3 B). These 38 genes correspond to 32 human orthologues, which include three alleles annotated in COSMIC as cancer genes (Futreal et al., 2004): *TET2*, *PTPN11*, and *THRAP3*.

Expression of AML1-ETO in *Tet2*-null cells generates a novel model of t(8;21)$^+$ AML

The variants detected in *TET2* in AML patients include nonsense, frameshift, and missense mutations within conserved domains, consistent with loss of TET2 enzymatic function (Table S1). Notably, 3 of the 29 t(8;21)$^+$ AML patients enrolled in the ECOG E1900 trial (Patel et al., 2012) harbored *TET2* mutations (Fig. 3 C and Table S2). In vivo, monoallelic or biallelic loss of *Tet2* in the hematopoietic compartment of mice results in myeloproliferation and extramedullary hematopoiesis but not AML (Li et al., 2011; Moran-Crusio et al., 2011).

To determine whether loss of *Tet2* can cooperate with AML1-ETO in vivo, we transduced bone marrow cells from *Vav-Cre*$^+$ *Tet2*$^{f/f}$ (*Tet2* KO) mice with AML1-ETO or AML1-ETO9 and transplanted the cells into lethally irradiated recipients. Mice transplanted with AML1-ETO–expressing *Tet2* KO cells developed fully penetrant leukemia, whereas mice transplanted with AML1-ETO9a–expressing *Tet2* KO cells developed a significantly accelerated leukemia with a median latency of 118 d ($P < 0.0001$; Fig. 4 A). At euthanasia, leukemic recipients had anemia, thrombocytopenia, elevated white blood cell counts (Fig. 4 B), and blast cell infiltration into the liver and spleen, with consequent splenomegaly (Fig. 4, C and D). The GFP$^+$ blast cells are lineage negative, SCA-1 positive or negative, and c-Kit positive (Fig. 4 E).

The observed cooperativity between *Tet2* loss and AML1-ETO in vivo implicates *TET2* loss-of-function mutations in t(8;21)$^+$ AML patients as functional cooperating events and challenges the traditional "two-hit hypothesis" of AML, which posits that AML1-ETO commonly cooperates with events that activate oncogenic signaling (Kelly and Gilliland, 2002). Our data support an expanded version of this hypothesis, in which a third class of events capable of enhancing self-renewal are capable of cooperating with AML1-ETO. Given that neomorphic mutations in IDH1/2 and loss-of-function mutations in WT1 also attenuate TET2 function and reduce DNA hydroxymethylation in vivo (Figueroa et al., 2010; Rampal et al., 2014), it will be important to determine whether altered DNA hydroxymethylation is a common pathogenetic event in AML1-ETO$^+$ AML and whether AML1-ETO$^+$ leukemias with concurrent mutations in epigenetic regulators have a distinct epigenetic profile and/or a distinct response to epigenetic therapies.

Expression of AML1-ETO with PTPN11 D61Y generates a novel model of t(8;21)$^+$ AML

The PTPN11 mutations that we observe in human and mouse AML occur within highly conserved regions of PTPN11 critical to phosphatase activity and the stimulation of RAS signaling (Fig. 3 D and Table S3; Yu et al., 2014). Previous studies have shown that mice expressing the constitutively active D61Y mutation (*Ptpn11*^{D61Y}) develop a fatal myeloproliferative neoplasm. However, bone marrow cells from these mice fail to engraft beyond 20 wk in transplant recipients and do not induce AML (Chan et al., 2009). We therefore transduced bone marrow cells from *Ptpn11*^{D61Y} mice with AML1-ETO and transplanted the cells into lethally irradiated recipients. Mice expressing both alleles developed fatal AML (Fig. 5 A). At euthanasia, leukemic mice had elevated white blood cell counts, anemia, thrombocytopenia (Fig. 5 B), and blast cell accumulation in the bone marrow, liver, and spleen (Fig. 5,

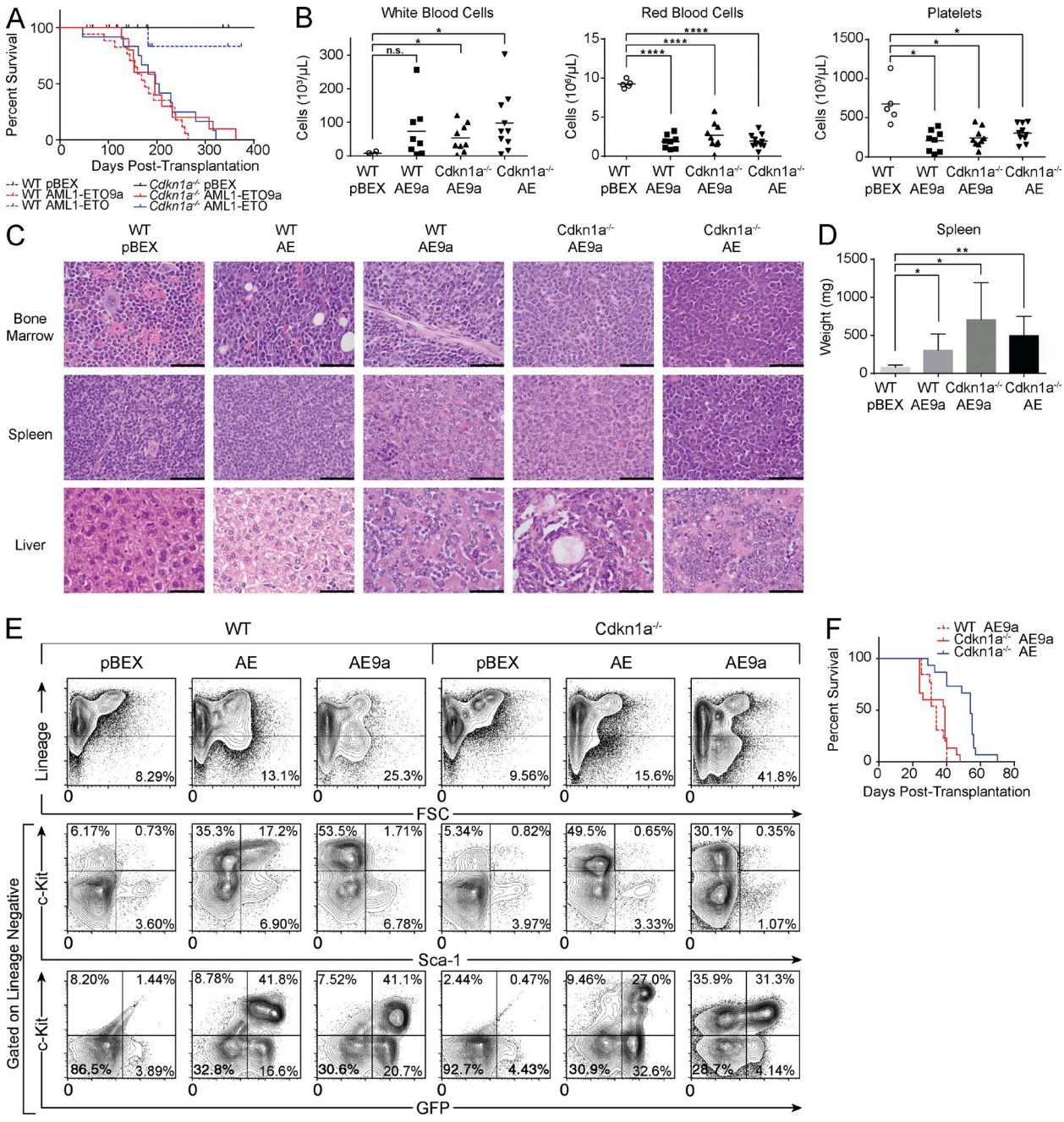

Figure 1. **Mouse models of AML1-ETO–driven leukemogenesis are phenotypically similar.** (A) Kaplan-Meier plot of mouse survival after transplantation with cells transduced with the given vector. WT pBEX (n = 12); WT AE9a (AML1-ETO9a; n = 17); WT AE (AML1-ETO; n = 17); *Cdkn1a*$^{-/-}$ pBEX (n = 11); *Cdkn1a*$^{-/-}$ AE9a (n = 10); *Cdkn1a*$^{-/-}$ AE (n = 12). (B) Peripheral blood counts of leukemic mice (from left to right, n = 8, n = 9, and n = 10) and controls (n = 5). Horizontal bars represent mean. (C) Representative hematoxylin and eosin staining (n = 3). Bars, 50 µm. (D) At euthanasia, leukemic mice exhibit significant splenomegaly compared with controls. WT pBEX (n = 2); WT AE9a (n = 8); *Cdkn1a*$^{-/-}$ AE9a (n = 5); *Cdkn1a*$^{-/-}$ AE (n = 7). Error bars represent the standard deviation from the mean. (B and D) P-values were generated using the Student's t test: *, P < 0.05; **, P < 0.01; ****, P < 0.0001; n.s., not significant. (E) Representative flow cytometry analysis of the bone marrow of transplant recipients (n = 10). (F) Kaplan-Meier plot of mouse survival after transplantation with 2 × 10^6 leukemic spleen cells. WT AE9a (n = 15); *Cdkn1a*$^{-/-}$ AE9a (n = 13); *Cdkn1a*$^{-/-}$ AE (n = 15).

C and D). These GFP$^+$ blasts were Sca-1 negative and c-Kit positive (Fig. 5 E) and capable of transmitting the disease into secondary recipients (not depicted).

The observation that AML1-ETO can cooperate with PTPN11 D61Y is more consistent with the two-hit hypothesis and implicates a novel member of the RAS signaling

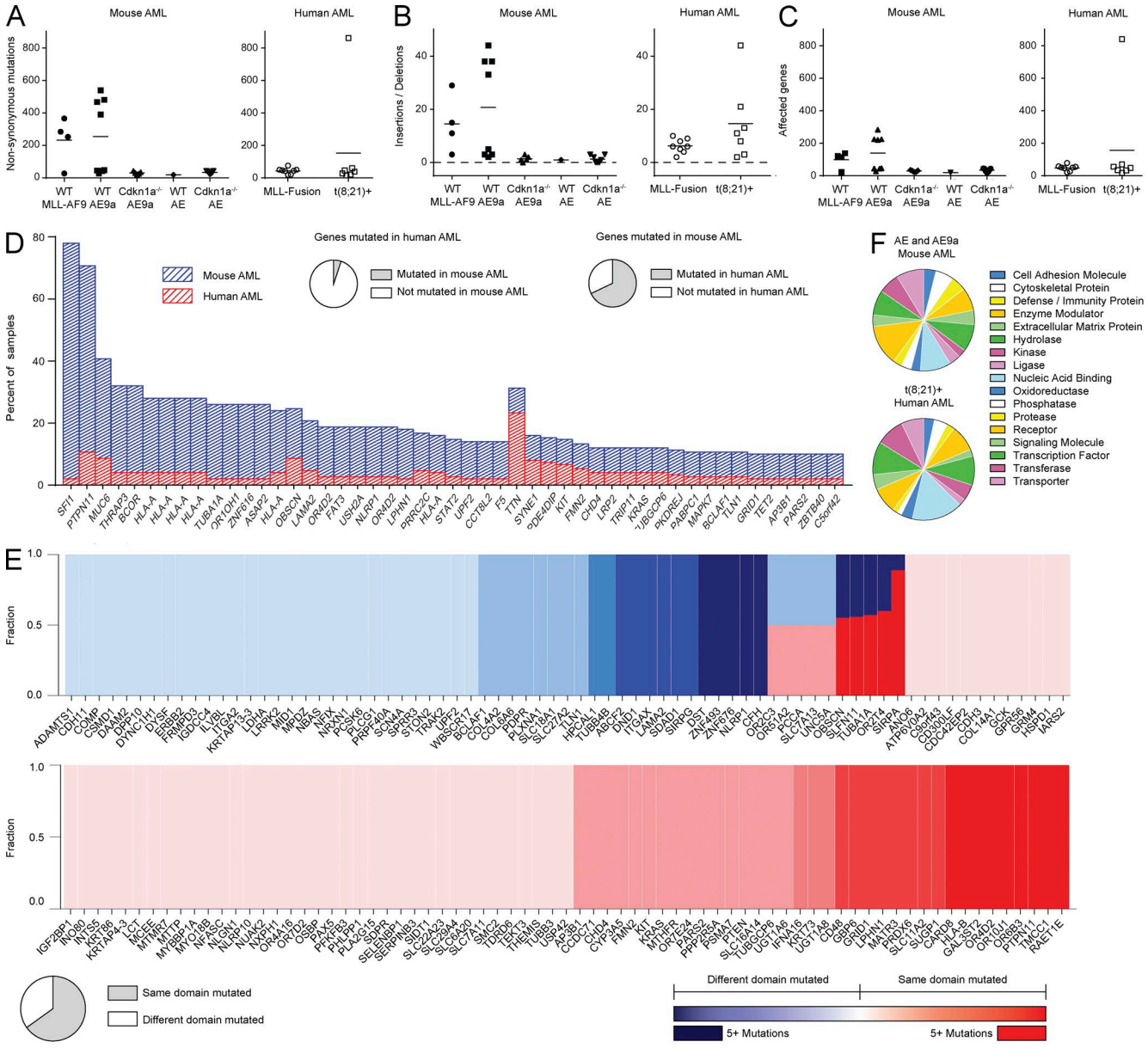

Figure 2. **Mouse AML reflects the mutational landscape of human AML.** (A–C) The number of nonsynonymous mutations (A), insertion and deletion events (B), and the number of genes harboring nonsynonymous, insertion, or deletion events in leukemic mice and human AML patients (C). Horizontal bars represent mean. (D) A stacked plot of the genes that are mutated in ≥2% of human AML samples and ≥8% of mouse AML samples. 67.90% of genes mutated in leukemic mice are also mutated in human AML patients, whereas only 5.07% of genes with a protein-coding mutation in AML patients are also mutated in leukemic mice. This enrichment is significant (hypergeometric $P \leq 4.26 \times 10^{-20}$). (E) Of the genes that harbor protein-coding mutations in both leukemic mice and human AML patients, the fraction of protein domains that are mutated in both species (red) or in only one species (blue) is depicted. The color intensity increases with the number of mutations in a given protein domain. 65.07% of these protein domains are mutated in both species, demonstrating enrichment (hypergeometric $P \leq 4.23 \times 10^{-3}$). Domains similarly affected are recurrently mutated (Spearman correlation of domain p-values $r = 0.53$, binomial $P \leq 2.73 \times 10^{-8}$). (F) The frequencies with which various protein classes are mutated in t(8;21)$^+$ mouse and human AML are not significantly different ($P = 0.327$, a transformed value of the Pillai-Bartlett statistic from a MANOVA model).

cascade in leukemogenesis. Although RAS mutations occur in 8–10% of AML1-ETO$^+$ AML patients (Peterson et al., 2007a), PTPN11 mutations may be a rare event (Loh et al., 2004). Previous studies pairing AML1-ETO with activating RAS mutations in vivo have had mixed results (Flotho, C. et al. 2004. 46th Annual Meeting of the American Society of Hematology. Poster #770-II; Chou et al., 2011; Zhao et al., 2014). Our data showing that PTPN11 D61Y is capable

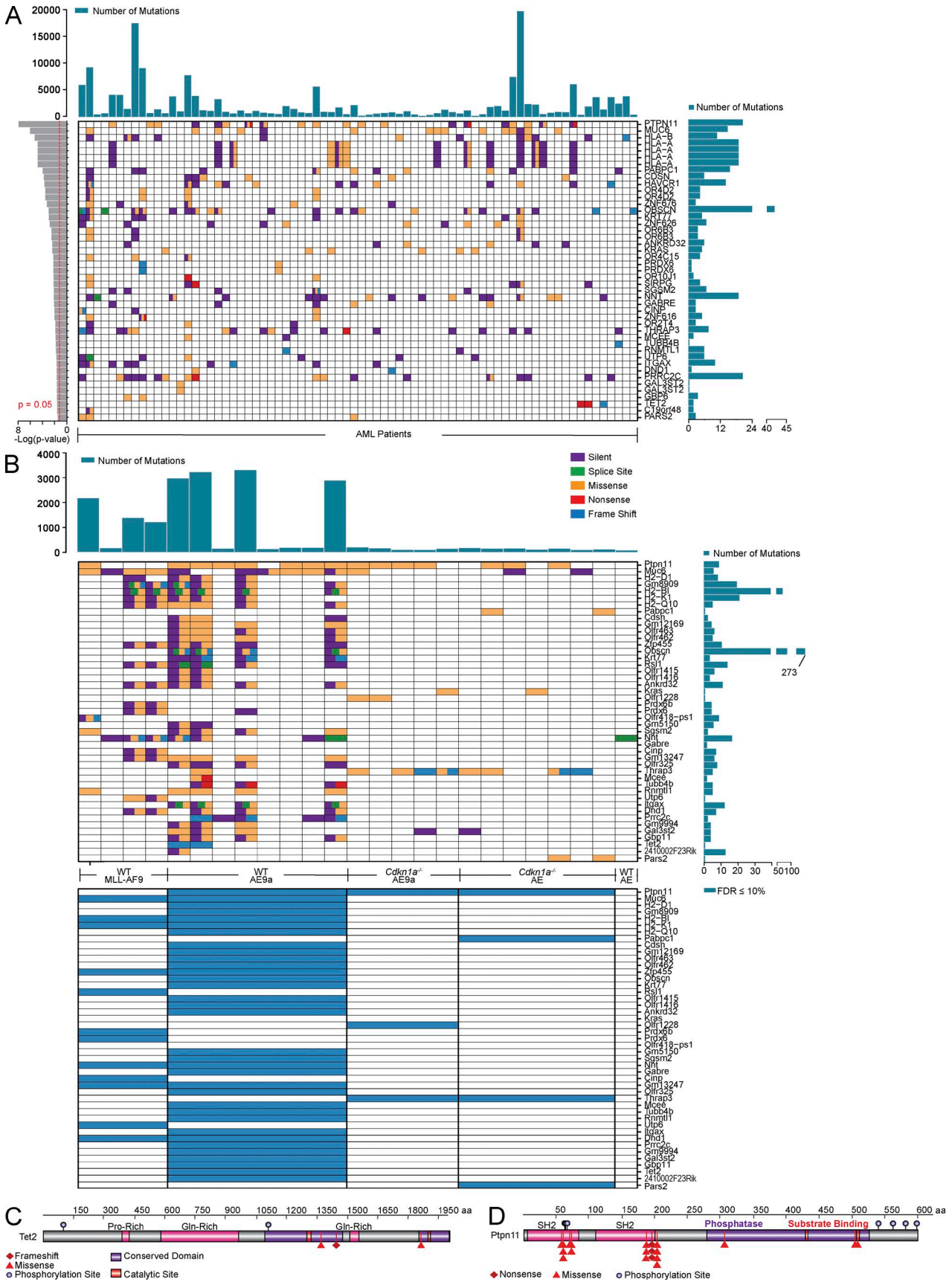

of cooperating with AML1-ETO suggests that MAPK-directed therapies should be investigated in these genetically defined t(8;21)$^+$ AML subsets.

In each of these newly developed mouse models of AML1-ETO–driven AML, the possibility remains that a third hit has been acquired that is necessary for disease initiation. Fortunately, our integrated approach can be applied to these leukemias such that those events are identified and credentialed in an iterative manner. Like previous studies in mouse solid tumors (Maser et al., 2007) and acute promyelocytic leukemia (Wartman et al., 2011), our data suggest that systematic comparisons of mutational patterns in mouse and human malignancies represent a powerful means of identifying cooperating disease alleles with mechanistic and therapeutic relevance.

MATERIALS AND METHODS

Construction of expression vectors and virus production. The cDNAs encoding AML1-ETO or AML1-ETO9a were digested with NotI and cloned into the NotI multiple cloning site of the MSCV-IRES-BEX plasmid (pBEX), upstream of the IRES and blue-excited GFP motifs. pBEX differs from the previously described MigR1 plasmid by featuring cDNA for enhanced GFP that has been altered such that it can be distinguished from violet-excited GFP (Anderson et al., 1996). To produce retrovirus capable of expressing AML1-ETO or AML1-ETO9a, 293T cells were cotransfected with a pBEX plasmid and MCV-Ecopac via calcium phosphate precipitation.

Fetal liver and bone marrow transduction and transplantation. Fetal liver cells were harvested from embryonic day (E) 14.5 WT (The Jackson Laboratory) or *Cdkn1a*$^{-/-}$ (provided by T. Jacks, The David H. Koch Institute for Integrative Cancer Research at MIT, Cambridge, MA) C57BL/6 embryos, whereas bone marrow cells from adult *Vav-Cre*$^+$ or *Vav-Cre*$^+$*Tet2*$^{f/f}$ C57BL/6 mice (Moran-Crusio et al., 2011) were harvested 6 d after intraperitoneal administration of 200 mg/kg 5-fluorouracil (Sigma-Aldrich). Bone marrow cells were harvested from 9-wk-old *Mx1-Cre*$^+$ or *Ptpn11*^{D61Y} mice that had been treated at 3 wk with poly(I:C) as previously published (Chan et al., 2009). Harvested cells were cultured in RPMI media supplemented with 10% fetal bovine serum, 10 ng/ml IL-3, 10 ng/ml IL-6, and 100 ng/ml stem cell factor (PeproTech) before transplantation, with 8 µg/ml polybrene (Sigma-Aldrich) added during spinoculation. Transduced cells were transplanted into 8–10-wk-old female C57BL/6 recipient mice by tail vein injection after the recipient mice had been lethally irradiated with 950 cGy, given in a split dose separated by 3 h. Procedures performed on these mice were approved by the Institutional Animal Care and Use Committee of Memorial Sloan Kettering Cancer Center.

Exome sequencing. Genomic DNA from GFP$^+$ mouse spleen cells or mouse tail tissue was isolated using phenol-chloroform extraction. Exome capture was performed using the SureSelect Mouse All Exon kit (Agilent Technologies), and sequencing was performed using an Illumina platform. Approximately 80 million reads per sample were acquired after a paired-end run with 75 or 100 bp. Paired-end reads were aligned to the NCBIM37.67/mm9 mouse reference genome using the Burrows-Wheeler Aligner (BWA) aln v0.6.2 and processed using the best practices pipeline that included marking of duplicate reads by the use of Picard tools and realignment around indels and base recalibration via Genome Analysis Toolkit (GATK) v3.1.1. Somatic single nucleotide variants (SNVs) were called using muTect v1.1.4, Virmid v1.1.0, and Strelka v1.0.12 and somatic indels via SomaticIndelDetector v2.3.9 and Strelka. SNVs and indels were filtered using the default filtering criteria as implemented in each of the callers and annotated via snpEff and snpSift. In addition, all germline SNVs and indels identified in the 17 key mouse strains as part of the Mouse Genome Project (Keane et al., 2011) were filtered out of the call set. To compare our results with what has been previously discovered in human patients, we downloaded the BAM files for the 150 human AML exomes from The Cancer Genome Atlas project (Cancer Genome Atlas Research Network, 2013). For consistency, we extracted the reads from human exomes, reprocessed them, and called somatic variants using the same pipeline as for mouse exomes.

SMGs and domain analysis. SMGs were identified in mouse and human samples using the SMG module from Genome MuSiC v0.4. Homology between mouse and human genes was based on the mouse–human homologue list downloaded from The Jackson Laboratory website. FDRs were determined using the likelihood ratio test from the Genome MuSiC SMG module. We annotated proteins with protein domains from Pfam-A, a database of high-quality, manually curated protein families. We used the hmmscan algorithm from HMMER3.0 package to match protein sequences against the Pfam-A database.

Statistical analysis. Statistical significance between two groups was assessed using the Student's *t* test with Welch's correction: *, $P < 0.05$; **, $P < 0.01$; ***, $P < 0.001$; ****, $P < 0.0001$; n.s., not significant. The hypergeometric test was used to determine whether there was significant overlap

Figure 3. **SMGs in mouse AML identify SMGs in human AML that are potential AML1-ETO cooperating partners.** (A) The patients that harbor nonsynonymous mutations in genes that are significantly mutated in human AML (FDR ≤ 30%). (B) For the genes significantly mutated in human AML, the types of mutations present in mouse AML samples are depicted. Those genes that are significantly mutated in a given mouse AML group (FDR ≤ 10%) are highlighted in blue under the given group. (C) *TET2* mutations identified in t(8;21)$^+$ AML patients. (D) *PTPN11* mutations identified in AML patients.

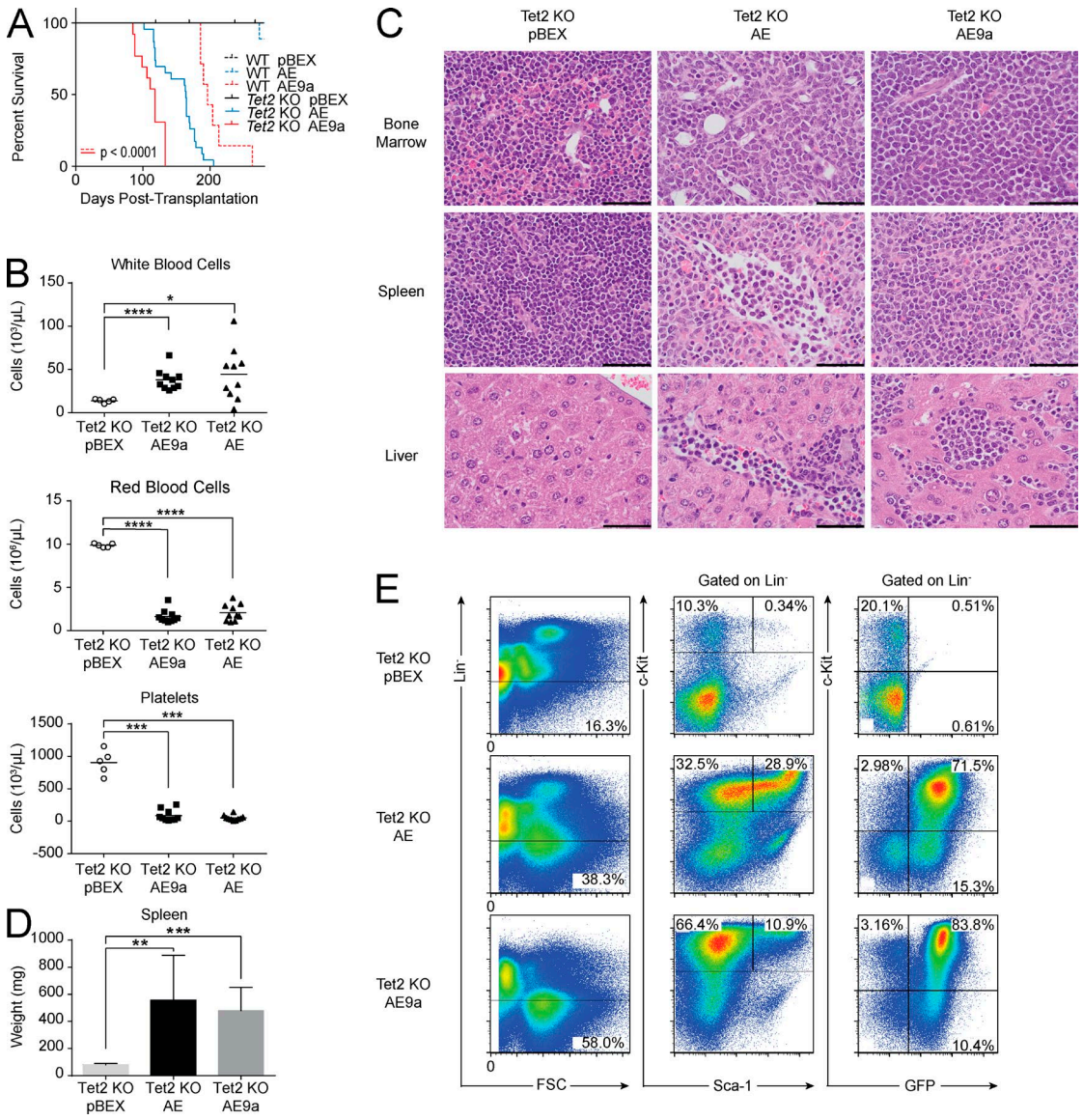

Figure 4. ***Tet2* loss cooperates with AML1-ETO to induce leukemia in vivo.** (A) Kaplan-Meier plot of mouse survival after transplantation with cells transduced with the given vector. WT pBEX ($n = 5$); WT AE ($n = 10$); WT AE9a ($n = 7$); *Tet2* KO pBEX ($n = 12$); *Tet2* KO AE ($n = 23$); *Tet2* KO AE9a ($n = 13$). *Tet2* loss significantly accelerates AE9a leukemias ($P < 0.0001$ using the Log-rank test). (B) Peripheral blood counts of mice transplanted with *Tet2* KO cells expressing AE9a ($n = 10$), AE ($n = 10$), or pBEX ($n = 5$). Horizontal bars represent mean. (C) Representative hematoxylin and eosin staining ($n = 3$). Bars, 50 µm. (D) At euthanasia, leukemic mice exhibit significant splenomegaly compared with controls. *Tet2* KO pBEX ($n = 2$); *Tet2* KO AE ($n = 9$); *Tet2* KO AE9a ($n = 9$). Error bars represent the standard deviation from the mean. (B and D) P-values were generated using the Student's *t* test: *, $P < 0.05$; **, $P < 0.01$; ***, $P < 0.001$; ****, $P < 0.0001$. (E) Representative flow cytometry analysis of the bone marrow of transplant recipients ($n = 10$).

in the genes that were mutated in mouse and human AML, as well as whether there was significant overlap in the protein domains that were affected in genes mutated in both mouse and human AML. The significance of recurrently mutated protein domains was determined using the binomial test, where p = length of domain (in AA)/length of protein (in AA). To determine whether mouse leukemias were significantly different from human leukemias with respect to the frequency with which all protein classes were affected by gene mutations, protein classes annotated using PANTHER (Mi et al., 2013) were compared across the two groups using the Pillai-Bartlett statistic from a multivariate ANOVA (MANOVA) model. The corresponding p-values were computed from a transformed value of the test statistic which has an approximate F distribution. All calculations were performed using R version 3.0.

Flow cytometry. To determine the immunophenotype of normal and leukemic populations, cells were stained with a panel of antibodies against lineage markers, each of which was

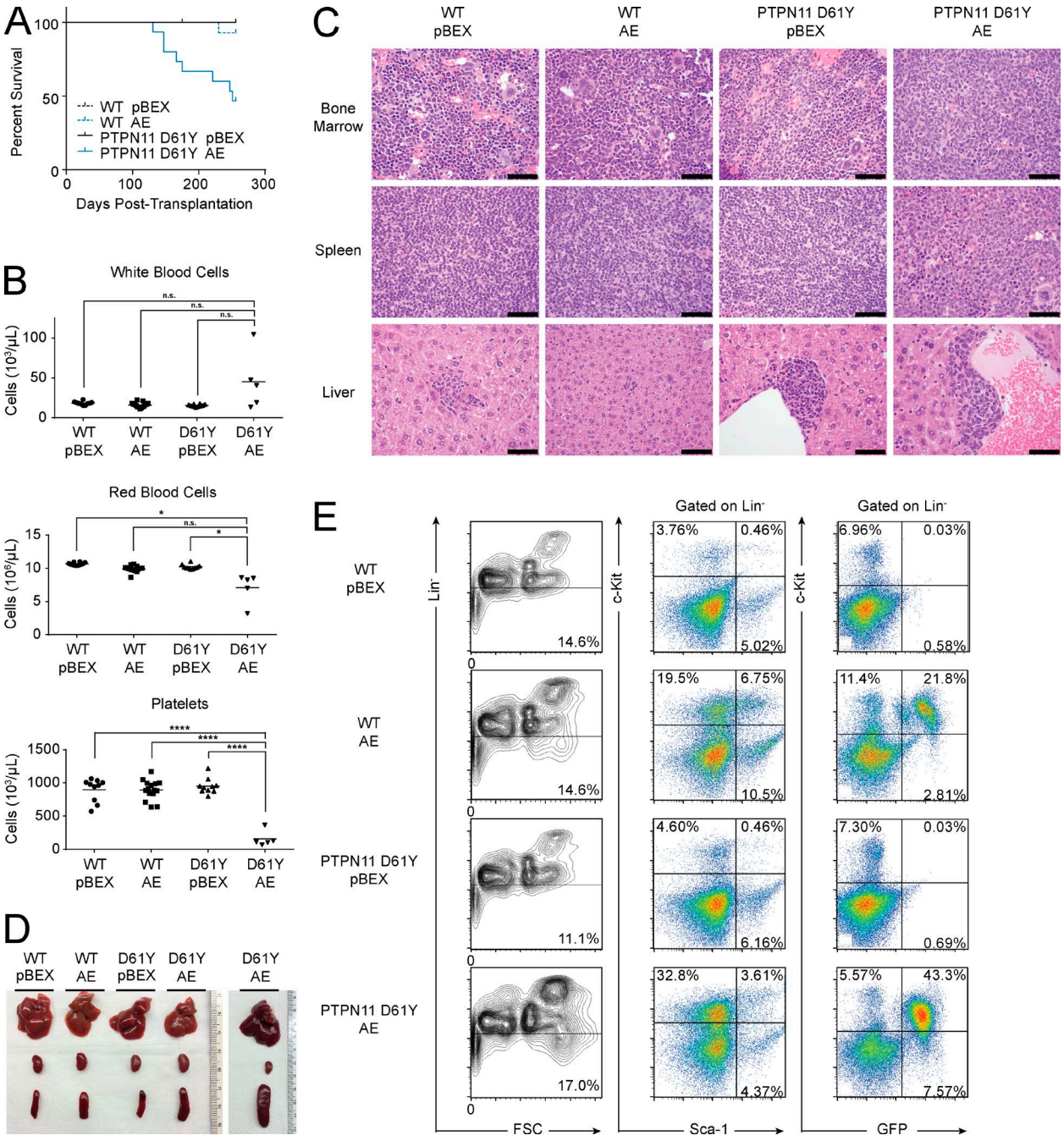

Figure 5. **PTPN11 D61Y cooperates with AML1-ETO to induce leukemia in vivo.** (A) Kaplan-Meier plot of mouse survival after transplantation with cells transduced with the given vector. WT pBEX (n = 10); WT AE (n = 15); PTPN11 D61Y pBEX (n = 10); PTPN11 D61Y AE (n = 15). (B) Peripheral blood counts at euthanasia of leukemic PTPN11 D61Y AE mice (n = 5), as well as controls (from left to right, n = 10, n = 15, and n = 10). Horizontal bars represent mean. P-values were generated using the Student's t test: *, $P < 0.05$; ****, $P < 0.0001$; n.s., not significant. (C) Representative hematoxylin and eosin staining (n = 3). Bars, 50 µm. (D) At euthanasia, leukemic mice exhibit splenomegaly. From top to bottom: liver, kidney, and spleen. (E) Representative flow cytometry analysis of the bone marrow of transplant recipients (n = 3).

conjugated to APC-Cy7: CD3, CD4, CD11b, CD19, CD45R, Gr-1, NK1.1, and TER119. Cells were also stained with anti-CD117 (c-KIT) and anti–SCA-1, conjugated to PE and PE-Cy7, respectively (BioLegend). Stained cells were analyzed using an LSR Fortessa or LSR II flow cytometer (BD), and data were analyzed using FlowJo software.

Online supplemental material. Table S1 lists the *TET2* mutations identified in AML patients from studies by the Cancer Genome Atlas Research Network (2013) and Patel et al. (2012). Table S2 provides statistics on the *TET2* mutations identified in AML patients from the Patel et al. (2012) study. Table S3 lists the *PTPN11* mutations identified in AML patients from the Cancer Genome Atlas Research Network (2013) study. Online supplemental material is available at http://www.jem.org/cgi/content/full/jem.20150524/DC1.

ACKNOWLEDGMENTS

The authors thank members of the Nimer, Levine, and Kharas laboratories for their suggestions and helpful comments regarding this work.

This work was funded by National Institutes of Health R01 grant CA 166835 to S.D. Nimer, by grant CA172636-01 to R.L. Levine, and by Memorial Sloan Kettering Cancer Center Support Grant/Core Grant P30 CA008748. R.L. Levine is a Scholar and A.H. Shih is a Special Fellow of the Leukemia and Lymphoma Society.

The authors declare no competing financial interests.

Submitted: 20 March 2015

Accepted: 13 November 2015

REFERENCES

Alcalay, M., N. Meani, V. Gelmetti, A. Fantozzi, M. Fagioli, A. Orleth, D. Riganelli, C. Sebastiani, E. Cappelli, C. Casciari, et al. 2003. Acute myeloid leukemia fusion proteins deregulate genes involved in stem cell maintenance and DNA repair. *J. Clin. Invest.* 112:1751–1761. http://dx.doi.org/10.1172/JCI17595

Anderson, M.T., I.M. Tjioe, M.C. Lorincz, D.R. Parks, L.A. Herzenberg, G.P. Nolan, and L.A. Herzenberg. 1996. Simultaneous fluorescence-activated cell sorter analysis of two distinct transcriptional elements within a single cell using engineered green fluorescent proteins. *Proc. Natl. Acad. Sci. USA.* 93:8508–8511. http://dx.doi.org/10.1073/pnas.93.16.8508

Cancer Genome Atlas Research Network. 2013. Genomic and epigenomic landscapes of adult de novo acute myeloid leukemia. *N. Engl. J. Med.* 368:2059–2074. http://dx.doi.org/10.1056/NEJMoa1301689

Chan, G., D. Kalaitzidis, T. Usenko, J.L. Kutok, W. Yang, M.G. Mohi, and B.G. Neel. 2009. Leukemogenic Ptpn11 causes fatal myeloproliferative disorder via cell-autonomous effects on multiple stages of hematopoiesis. *Blood.* 113:4414–4424. http://dx.doi.org/10.1182/blood-2008-10-182626

Chou, F.-S., M. Wunderlich, A. Griesinger, and J.C. Mulloy. 2011. N-Ras^{G12D} induces features of stepwise transformation in preleukemic human umbilical cord blood cultures expressing the AML1-ETO fusion gene. *Blood.* 117:2237–2240. http://dx.doi.org/10.1182/blood-2010-01-264119

Figueroa, M.E., O. Abdel-Wahab, C. Lu, P.S. Ward, J. Patel, A. Shih, Y. Li, N. Bhagwat, A. Vasanthakumar, H.F. Fernandez, et al. 2010. Leukemic IDH1 and IDH2 mutations result in a hypermethylation phenotype, disrupt TET2 function, and impair hematopoietic differentiation. *Cancer Cell.* 18:553–567. http://dx.doi.org/10.1016/j.ccr.2010.11.015

Futreal, P.A., L. Coin, M. Marshall, T. Down, T. Hubbard, R. Wooster, N. Rahman, and M.R. Stratton. 2004. A census of human cancer genes. *Nat. Rev. Cancer.* 4:177–183. http://dx.doi.org/10.1038/nrc1299

Higuchi, M., D. O'Brien, P. Kumaravelu, N. Lenny, E.-J. Yeoh, and J.R. Downing. 2002. Expression of a conditional AML1-ETO oncogene bypasses embryonic lethality and establishes a murine model of human t(8;21) acute myeloid leukemia. *Cancer Cell.* 1:63–74. http://dx.doi.org/10.1016/S1535-6108(02)00016-8

Keane, T.M., L. Goodstadt, P. Danecek, M.A. White, K. Wong, B. Yalcin, A. Heger, A. Agam, G. Slater, M. Goodson, et al. 2011. Mouse genomic variation and its effect on phenotypes and gene regulation. *Nature.* 477:289–294. http://dx.doi.org/10.1038/nature10413

Kelly, L.M., and D.G. Gilliland. 2002. Genetics of myeloid leukemias. *Annu. Rev. Genomics Hum. Genet.* 3:179–198. http://dx.doi.org/10.1146/annurev.genom.3.032802.115046

Li, Z., X. Cai, C.L. Cai, J. Wang, W. Zhang, B.E. Petersen, F.C. Yang, and M. Xu. 2011. Deletion of Tet2 in mice leads to dysregulated hematopoietic stem cells and subsequent development of myeloid malignancies. *Blood.* 118:4509–4518. http://dx.doi.org/10.1182/blood-2010-12-325241

Loh, M.L., M.G. Reynolds, S. Vattikuti, R.B. Gerbing, T.A. Alonzo, E. Carlson, J.W. Cheng, C.M. Lee, B.J. Lange, and S. Meshinchi. Children's Cancer Group. 2004. PTPN11 mutations in pediatric patients with acute myeloid leukemia: results from the Children's Cancer Group. *Leukemia.* 18:1831–1834. http://dx.doi.org/10.1038/sj.leu.2403492

Maser, R.S., B. Choudhury, P.J. Campbell, B. Feng, K.-K. Wong, A. Protopopov, J. O'Neil, A. Gutierrez, E. Ivanova, I. Perna, et al. 2007. Chromosomally unstable mouse tumours have genomic alterations similar to diverse human cancers. *Nature.* 447:966–971. http://dx.doi.org/10.1038/nature05886

McDonald, E.R. III, G.S. Wu, T. Waldman, and W.S. El-Deiry. 1996. Repair defect in p21 WAF1/CIP1 −/− human cancer cells. *Cancer Res.* 56:2250–2255.

Mi, H., A. Muruganujan, and P.D. Thomas. 2013. PANTHER in 2013: modeling the evolution of gene function, and other gene attributes, in the context of phylogenetic trees. *Nucleic Acids Res.* 41:D377–D386. http://dx.doi.org/10.1093/nar/gks1118

Moran-Crusio, K., L. Reavie, A. Shih, O. Abdel-Wahab, D. Ndiaye-Lobry, C. Lobry, M.E. Figueroa, A. Vasanthakumar, J. Patel, X. Zhao, et al. 2011. Tet2 loss leads to increased hematopoietic stem cell self-renewal and myeloid transformation. *Cancer Cell.* 20:11–24. http://dx.doi.org/10.1016/j.ccr.2011.06.001

Müller, A.M., J. Duque, J.A. Shizuru, and M. Lübbert. 2008. Complementing mutations in core binding factor leukemias: from mouse models to clinical applications. *Oncogene.* 27:5759–5773. http://dx.doi.org/10.1038/onc.2008.196

Patel, J.P., M. Gönen, M.E. Figueroa, H. Fernandez, Z. Sun, J. Racevskis, P. Van Vlierberghe, I. Dolgalev, S. Thomas, O. Aminova, et al. 2012. Prognostic relevance of integrated genetic profiling in acute myeloid leukemia. *N. Engl. J. Med.* 366:1079–1089. http://dx.doi.org/10.1056/NEJMoa1112304

Peterson, L.F., A. Boyapati, E.-Y. Ahn, J.R. Biggs, A.J. Okumura, M.-C. Lo, M. Yan, and D.-E. Zhang. 2007a. Acute myeloid leukemia with the 8q22;21q22 translocation: secondary mutational events and alternative t(8;21) transcripts. *Blood.* 110:799–805. http://dx.doi.org/10.1182/blood-2006-11-019265

Peterson, L.F., M. Yan, and D.-E. Zhang. 2007b. The p21Waf1 pathway is involved in blocking leukemogenesis by the t(8;21) fusion protein AML1-ETO. *Blood.* 109:4392–4398. http://dx.doi.org/10.1182/blood-2006-03-012575

Rampal, R., A. Alkalin, J. Madzo, A. Vasanthakumar, E. Pronier, J. Patel, Y. Li, J. Ahn, O. Abdel-Wahab, A. Shih, et al. 2014. DNA hydroxymethylation profiling reveals that WT1 mutations result in loss of TET2 function in acute myeloid leukemia. *Cell Reports.* 9:1841–1855. http://dx.doi.org/10.1016/j.celrep.2014.11.004

Shiohara, M., K. Koike, A. Komiyama, and H.P. Koeffler. 1997. p21WAF1 mutations and human malignancies. *Leuk. Lymphoma.* 26:35–41.

Stubbs, M.C., Y.M. Kim, A.V. Krivtsov, R.D. Wright, Z. Feng, J. Agarwal, A.L. Kung, and S.A. Armstrong. 2008. MLL-AF9 and FLT3 cooperation in acute myelogenous leukemia: development of a model for rapid therapeutic assessment. *Leukemia.* 22:66–77. http://dx.doi.org/10.1038/sj.leu.2404951

Wartman, L.D., D.E. Larson, Z. Xiang, L. Ding, K. Chen, L. Lin, P. Cahan, J.M. Klco, J.S. Welch, C. Li, et al. 2011. Sequencing a mouse acute

promyelocytic leukemia genome reveals genetic events relevant for disease progression. *J. Clin. Invest.* 121:1445–1455. http://dx.doi.org/10.1172/JCI45284

Yan, M., E. Kanbe, L.F. Peterson, A. Boyapati, Y. Miao, Y. Wang, I.-M. Chen, Z. Chen, J.D. Rowley, C.L. Willman, and D.-E. Zhang. 2006. A previously unidentified alternatively spliced isoform of t(8;21) transcript promotes leukemogenesis. *Nat. Med.* 12:945–949. http://dx.doi.org/10.1038/nm1443

Yu, Z.-H., R.-Y. Zhang, C.D. Walls, L. Chen, S. Zhang, L. Wu, S. Liu, and Z.-Y. Zhang. 2014. Molecular basis of gain-of-function LEOPARD syndrome-associated SHP2 mutations. *Biochemistry.* 53:4136–4151. http://dx.doi.org/10.1021/bi5002695

Zhao, S., Y. Zhang, K. Sha, Q. Tang, X. Yang, C. Yu, Z. Liu, W. Sun, L. Cai, C. Xu, and S. Cui. 2014. KRAS (G12D) cooperates with AML1/ETO to initiate a mouse model mimicking human acute myeloid leukemia. *Cell. Physiol. Biochem.* 33:78–87. http://dx.doi.org/10.1159/000356651